

Quantum Hall and Light Responses in a 2D Topological Semimetal

Sariah Al Saati and Karyn Le Hur¹

¹CPHT, CNRS, Institut Polytechnique de Paris, Route de Saclay, 91120 Palaiseau, France

We investigate the topological characteristics of a recently discovered class of semimetals in two dimensions on the honeycomb lattice. These semimetals reside at the transition between two distinct topological insulators, each existing in a nontrivial topological phase. As a result, these semimetals exhibit specific topological properties, including the presence of edge modes. In a preceding work, we demonstrated the topological robustness of this semimetal phase against disorder and interactions. In this work, we delve deeper into the semimetal's electronic properties, providing a precise calculation of its Hall conductivity and response to circularly polarized light, elaborating further on its bulk-edge correspondence leading to a half topological semimetal.

I. INTRODUCTION

Topological materials have emerged in the last decades as a remarkable class of materials that challenge conventional classifications of matter [1]. Among these materials, two-dimensional topological systems display unique electronic properties such as a quantized Hall conductivity [2, 3]. Moreover, unlike conventional insulators, which have an energy gap between their valence and conduction bands throughout the entire material, these quantum Hall-like systems possess states that display metallic behavior [4, 5] which are exclusively located on the edges allowing for the current to flow around the sample, protected from impurities and disorder.

At the heart of topological aspects in these condensed-matter systems is the nontrivial nature of the wavefunction in reciprocal space associated to the band structure of a crystal. Indeed, one of the key theoretical concepts underlying the study of topological matter is the notion of topological invariants which have direct consequences on the dynamics of the material. The main topological invariant of interest is the Chern number associated to the Brillouin Zone of the material. Remarkably, this integer Chern number was found to be directly related to the Hall conductivity of the material, showing a unique quantized behavior in units of the fundamental constant e^2/h [3, 6], accessible in quantum transport experiments. This topological number was also found to be equivalently accessible from the response of the material to circularly polarized light [7–9]. This topological response to circularly polarized light can also be equivalently resolved locally within the Brillouin zone [10].

Quantum spin Hall insulators are two-dimensional topological insulators which have gained prominence in the last two decades [11, 12]. Quantum spin Hall insulators are characterized by the presence of the spin Hall effect, where an electric current induces a transverse spin current due to intrinsic spin-orbit coupling. These spin Hall systems are most often theoretically described by two spin-polarized subsystems, called spin channels, which are related through time-reversal symmetry. A specific example is shown in Fig. 1 for the case of the Kane-Mele model [13, 14] in which the spin of the electron is a well defined quantum number labelling distinct

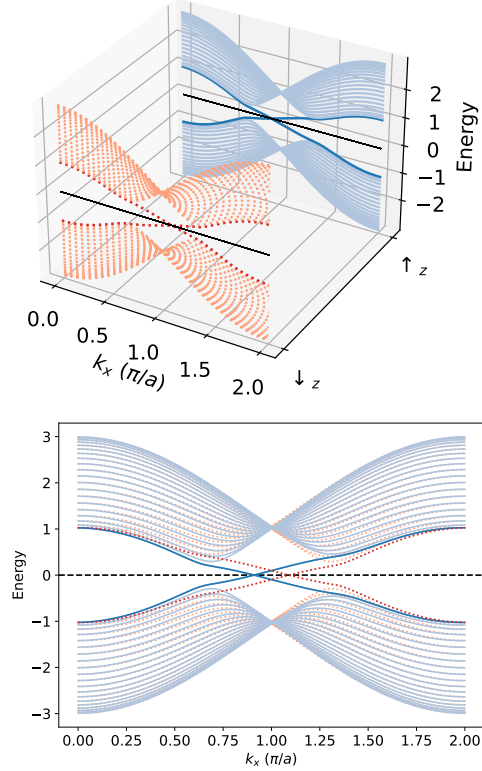


Figure 1. Color online: (Above) One-dimensional energy bands of the Kane-Mele model in the quantum spin Hall phase for the two spin polarizations of an electron, related through time-reversal symmetry. The spin polarization is shown in the third direction. (Bottom) Resulting energy bands in the momentum-Energy axis. Energies are measured in units of t for the different figures.

energy bands. In this model, each spin channel hosts oppositely directed edge modes, referring then to the quantum spin Hall effect. This description in terms of counter-propagating spin channels is also valid for the Bernevig-Hughes-Zhang model [15]. The system then hosts a zero total Chern number and is equivalently described through a \mathbb{Z}_2 topological spin Chern number related to the structure of the quantum spin Hall current at the edges [13, 16]. Circularly polarized light can measure this topological \mathbb{Z}_2 invariant related to the quantum spin

Hall effect [10] and the parity symmetry [17] with a perfect quantization at the Dirac points on the honeycomb lattice associated to the zeros of the Pfaffian [14].

The classification of topological properties in terms of two distinct Pauli matrices, e.g. related to the two sublattices on the honeycomb lattice and to the two spin polarizations of an electron in the Kane-Mele model, was at the heart of our recent publication [18] in which we describe a possible generalization of nontrivial topological properties and robustness towards a specific class of two-dimensional topological semimetals. The first hints pointing at the topological nature of this semimetal came from an earlier study made in our group on the general framework of topological spheres' models [19], and in which this topological semimetal was found to sit at a transition between two topologically distinct but still non trivial phases of the system. This semimetal was then understood to host two independent copies of the Haldane model [20] as in the Kane-Mele model, however in this case the two copies hosted the same topology but each was partially filled differently. As such, this semimetal was found to host robust edge modes characteristics of topological materials, giving rise to its non trivial topological nature as a semimetal. The robust edge mode is polarized along x direction which has then a one-half probability to reside in each plane for the bilayer model [19] or to be polarized along z direction for the one-layer graphene model [18].

The question of the topological classification of the semimetals is still an open question to this day [21], related to a possible generalization of the Thouless-Kohmoto-Nightingale-denNijs (TKNN) formula [3] for systems with a Fermi surface [22]. Indeed, for topological insulators, this formula expresses a dynamical property of the system (its Hall conductance) as a function of a topological property of the wavefunction of the ground state (its Chern number in reciprocal space). Several schemes can then be adopted in order to find a topological classification for semimetals, taking an inspiration from the existing classification for insulators. A first strategy would be to investigate in the gapless band structure of the semimetal possible candidates for topological invariants [23] but these invariants may not correspond to directly accessible experimental observables in terms of electronic transport. A second approach would be to discuss the topological properties of the corresponding insulators if the gap of the concerned semimetal opened and made infinitesimally small [24, 25] opening this way the field of approximate symmetries. A third approach, as done in the present paper, would consist to investigate in the band structure of the semimetal possible signatures of the topological nature of the bands. Yet, taking the point of view of the first approach, we will show how the protocols of [9, 10, 26] to analyze the response to circularly polarized light locally within the Brillouin zone can also provide a meaningful information of the topological response of the quantum Hall conductivity related to a half topological semimetal [19, 27]. This approach is restricted

here to a specific class of models which are built out of two or more independent copies of the Haldane model, but this class of models is still of major interest nowadays for this discussion to bring many interesting insights to the field of topology in condensed matter physics.

In this context, the aim of the present paper is thus to provide a clear evaluation of the quantum Hall conductivity and of the responses to circularly polarized light for this protected topological semimetal discussing in greater details its bulk-edge correspondence. The article is organized as follows. In Sec. II, we remind main properties of the topological semimetal. In Sec. III, we present the derivation of the quantum Hall conductivity for this system. In Sec. IV, we derive a topological response through circularly polarized light locally from the Dirac points within the Brillouin zone. In Sec. V, we discuss the bulk-edge correspondence and possible applications through Angle-Resolved Photoemission Electron Spectroscopy (ARPES), and formulate general remarks on this theoretical scheme. Then, in Sec. VI, we summarize our findings.

II. PROTECTED TOPOLOGICAL SEMIMETAL

The model of the semimetal we are interested in can be realized in a single layer of graphene [18]. This model relies on the presence of an Haldane model associated to the two spin polarizations of an electron. We include the presence of a magnetic field, such that its direction is fixed parallel to the layer to induce Zeeman effects. The energy bands of the system will be then classified according to the two spin polarizations of an electron along x direction. In the recent years, there have been many developments of proximity-induced topological phases of matter [28–31] and in particular on graphene/Transition-metal dichalcogenide (TMD) heterostructures [32, 33] with easily tunable parameters. Therefore, we can anticipate that there will be various equivalent ways to realize this topological semimetal in two dimensions through two sets of Pauli matrices related to the physics of heterostructures. The Hamiltonian of the two-dimensional (2D) topological semimetal can be written in tight-binding formalism in reciprocal space as [18]

$$\mathcal{H} = \sum_{\mathbf{k} \in BZ} \psi^\dagger(\mathbf{k}) \mathcal{H}(\mathbf{k}) \psi(\mathbf{k}) \quad (1)$$

with

$$\psi(\mathbf{k}) = (c_{A\mathbf{k}\uparrow}, c_{B\mathbf{k}\uparrow}, c_{A\mathbf{k}\downarrow}, c_{B\mathbf{k}\downarrow}) \quad (2)$$

$$\mathcal{H}(\mathbf{k}) = \mathbf{d}_{\mathbf{k}} \cdot \boldsymbol{\sigma} \otimes \mathbb{I} + r \mathbb{I} \otimes s_x, \quad (3)$$

where A and B label the two nonequivalent sites of the honeycomb lattice.

The Hamiltonian is written in terms of two sets of Pauli matrices: $\boldsymbol{\sigma}$ acting on the Hilbert space $\{|A\rangle; |B\rangle\}$

associated to the two sublattices A - B and \mathbf{s} acting on $\{|\uparrow_z\rangle; |\downarrow_z\rangle\}$ linked to the two spin polarizations of an electron in the direction perpendicular to the graphene layer. In this way, Zeeman effects occur through the x spin-Pauli matrix. We recall here that the $d_x(\mathbf{k})$ and $d_y(\mathbf{k})$ terms in the Bloch hamiltonian describe the kinetic terms of graphene whereas the $d_z(\mathbf{k})$ term represents the topological term introduced first by Haldane in 1988 [20] giving rise to a mass inversion effect between the two Dirac points K and K' in the Brillouin zone, referring to the inversion of eigenstates related to the lower and upper energy bands when inverting the two Dirac points. From standard definitions, on the honeycomb lattice, we identify the following respective components of the $\mathbf{d}_{\mathbf{k}} = \mathbf{d}(\mathbf{k})$ vector

$$d_x(\mathbf{k}) = -t \sum_{i=1}^3 \cos(\mathbf{k} \cdot \boldsymbol{\delta}_i) \quad (4)$$

$$d_y(\mathbf{k}) = -t \sum_{i=1}^3 \sin(\mathbf{k} \cdot \boldsymbol{\delta}_i) \quad (5)$$

$$d_z(\mathbf{k}) = M + 2t_2 \sum_j \sin(\mathbf{k} \cdot \mathbf{b}_j), \quad (6)$$

where $t > 0$ represents the hopping amplitude between nearest-neighbours A and B , and $\boldsymbol{\delta}_i$ represents the three nearest-neighbour vectors linking these sites. For simplicity, we assume here that the second nearest-neighbor hopping term is purely imaginary and equal to it_2 (with $t_2 > 0$) in the Haldane model. This term is the one giving rise to topological properties in graphene, and can be implemented using circularly polarized light [18, 26] as achieved in recent years [34]. Then, \mathbf{b}_j are the three second-nearest neighbour vectors forming a triangle across a unit cell, and M is a parameter referring to a modulated potential or a Semenoff mass term [35], which can be implemented e.g. through the presence of a substrate forming a charge density wave. This term is indeed important to induce a different energy shift at the two Dirac points.

This hamiltonian can readily be diagonalized and the Bloch eigenvectors can be expressed in tensorial product of the eigenstates $|\pm\rangle = |\pm_{\mathbf{d}_{\mathbf{k}}}\rangle$ of the operator $\mathbf{d}_{\mathbf{k}} \cdot \boldsymbol{\sigma}$ with eigenvalues $\pm|\mathbf{d}_{\mathbf{k}}|$, tensored with the eigenvectors $|\uparrow_x\rangle$ of the operator s_x with eigenvalues ± 1 . The resulting four possibly overlapping bands are

$$E_{\downarrow_x, -}(\mathbf{k}) = -|\mathbf{d}_{\mathbf{k}}| - r \quad (7)$$

$$E_{\downarrow_x, +}(\mathbf{k}) = +|\mathbf{d}_{\mathbf{k}}| - r \quad (8)$$

$$E_{\uparrow_x, -}(\mathbf{k}) = -|\mathbf{d}_{\mathbf{k}}| + r \quad (9)$$

$$E_{\uparrow_x, +}(\mathbf{k}) = +|\mathbf{d}_{\mathbf{k}}| + r. \quad (10)$$

The semimetallic regime is reached when the two middle bands overlap forming a closed one-dimensional Fermi surface denoted as nodal ring. An important prerequisite to observe the formation of a nodal metallic Fermi liquid is that when solving the equation $\mathcal{H}^2(\mathbf{k}) = 0 = (-r + |\mathbf{d}|)^2$

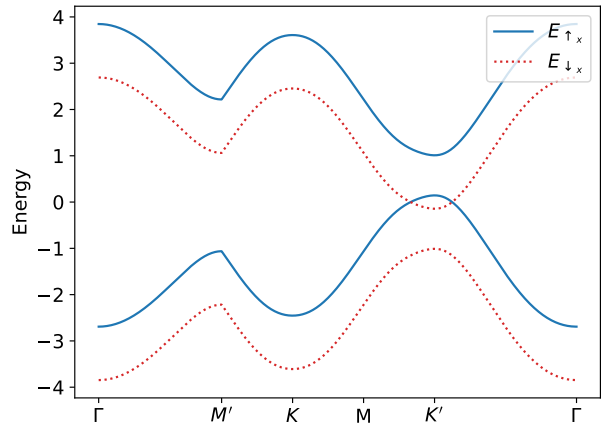


Figure 2. Color Online: Two-dimensional band structure of the system for a chosen path in the Brillouin zone with the spin polarizations associated to the energy bands shown in distinct colors. The parameters chosen for all panels are $M = 3\sqrt{3}t/4$, $r = t/\sqrt{3}$, $t_2 = t/3$ with lattice spacing $a = 1$. Results can be generalized as long as Eq. (11) is satisfied.

this leads to two degenerate solutions corresponding to the two eigenstates $|\uparrow_x\rangle \otimes |-\rangle$ and $|\downarrow_x\rangle \otimes |+\rangle$ such that $2r\mathbf{d} \cdot \boldsymbol{\sigma} \otimes s_x = -2r|\mathbf{d}|$.

The existence of this nodal ring giving the property of semimetal in addition to the topological properties is largely due to the \mathbb{Z}_2 inversion symmetry in the spin state $|\uparrow_z\rangle \leftrightarrow |\downarrow_z\rangle$ in the Hamiltonian (such that s_x commutes with the Hamiltonian) protecting it [18]. Indeed, the system is invariant under inversion of these spin polarizations and it was found that disorder and interactions do not lead to symmetry-breaking terms in the hamiltonian, such that the crossing between the two middle bands is preserved and no gap is opened. Indeed, mixing terms between the two middle bands are not likely to occur as these two bands are doubly orthogonal, firstly in the graphene site sector $|\pm\rangle$ of the wavefunction and secondly in the spin polarization sector $|\uparrow_x\rangle$ of the wavefunction. Instead, disorder and interactions add up to renormalize the magnetic field parameter $r \mapsto \tilde{r}$ for which the topological nodal ring semimetal is stable as long as [18]

$$3\sqrt{3}t_2 - M \leq \tilde{r} < 3\sqrt{3}t_2 + M. \quad (11)$$

The parameter \tilde{r} can be viewed as a small renormalization effect of the transverse magnetic field as a result of interactions which can be elegantly taken care of through a variational stochastic approach which can be successfully applied to interacting topological models [9, 36, 37] in quantitative agreement with numerical methods [38, 39]. Hereafter, we investigate in further details the expression of the Hall conductivity of the material to see how this can be related to topological invariants. This computation is in general not possible for crossing bands but we argue below that for this specific model, the evaluation is well defined and is free of divergences e.g. as a result of orthogonality of spin eigenstates

on both sides of the crossing regions.

For the Haldane model, or generally speaking a topological two-bands model, the responses to circularly polarized light reveal the same information as the quantum Hall conductivity [7–9] and this information can be in fact re-built from specific points in the Brillouin zone [10, 26], in particular the Dirac points.

We will then address this correspondence between quantum Hall conductivity and responses to circularly polarized light in Sec. IV and show that this yet reveals important signatures of topological properties of the semimetal from the Dirac points, e.g. through the topological invariant of the lowest-energy band, with a correspondence onto a half topological semimetal in the basis of \uparrow_z, \downarrow_z spin states.

III. KUBO FORMULA FOR HALL CONDUCTIVITY

In the linear response regime, the Kubo formula for the Hall conductivity of a 2D electron gas is given by [3]

$$\sigma^{xy} = ie^2\hbar \iint_{BZ} \frac{d^2\mathbf{k}}{(2\pi)^2} \sum_{n \neq m} \frac{f(E_n(\mathbf{k}))}{(E_n(\mathbf{k}) - E_m(\mathbf{k}))^2} \quad (12)$$

$$\times (\langle n\mathbf{k}|v^x|m\mathbf{k}\rangle\langle m\mathbf{k}|v^y|n\mathbf{k}\rangle - \langle n\mathbf{k}|v^y|m\mathbf{k}\rangle\langle m\mathbf{k}|v^x|n\mathbf{k}\rangle)$$

where the indices $n = \uparrow_x, \pm$ and $m = \downarrow_x, \pm'$ run over the four bands of the system, and $f(x) = \theta(x)$ is the Fermi-Dirac distribution function being equal to the Heaviside step function at zero temperature.

One may question the applicability of this formula in the semimetallic regime for which bands $\downarrow_x, +$ and $\uparrow_x, -$ cross zero energy such that $E_n(\mathbf{k}) - E_m(\mathbf{k}) = 0$, which seems to give us a diverging fraction in the expression of Eq. (13). Fortunately, this divergence is avoided by the fact that the current operator v^α does not couple these two bands as we have

$$v^\alpha = \frac{1}{\hbar} \partial_{k_\alpha} \mathcal{H} \otimes \mathbb{I}, \quad (13)$$

such that $\langle \uparrow_x, -|v^\alpha|\downarrow_x, +\rangle = 0$ identically over the entire Brillouin zone. Eq. (13) is thus well defined and we can rewrite this expression in terms of the integral of the Berry curvature over the Brillouin zone over all occupied states

$$\sigma^{xy} = \frac{e^2}{h} \iint_{BZ} \frac{d^2\mathbf{k}}{2\pi} \sum_n f(E_n(\mathbf{k})) \mathcal{B}_{n\mathbf{k}} \quad (14)$$

where the Berry curvature of band n is defined as [40]

$$\mathcal{B}_{n\mathbf{k}} = i(\partial_{k_x}\langle n|)\partial_{k_y}|n\rangle - i(\partial_{k_y}\langle n|)\partial_{k_x}|n\rangle. \quad (15)$$

In the semimetallic context, the contribution from the Fermi-Dirac distribution with the term $f(E_n(\mathbf{k}))$ appearing in Eq. (14) plays a major role as it constrains the integration to be performed only partially over the Brillouin

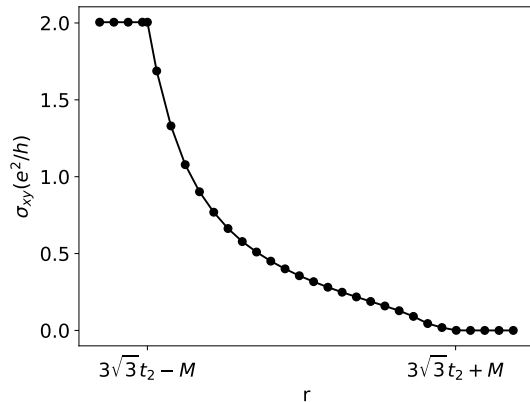


Figure 3. Numerical computation of the Hall conductivity of the topological semimetal for a given sample using the Kubo formula, as shown in Eq. (13). The total Hall conductivity gradually decreases from its quantized value $|\sigma^{xy}| = 2e^2/h$ in the topological insulating phase to $|\sigma^{xy}| = 0$ in the trivial insulating phase according to Eq. (29).

zone for the two middle bands $n = \downarrow_x, +$ and $n = \uparrow_x, -$ which correspond to two partially filled bands, while the integration is performed over the entire Brillouin zone for $n = \downarrow_x, -$ whose band is entirely filled. This expression gives

$$\sigma^{xy} = \frac{e^2}{h} \left(C_{\downarrow_x, -} + \hat{C}_{\uparrow_x, -} + \tilde{C}_{\downarrow_x, +} \right) \quad (16)$$

for which we have defined (hat and tilde symbols)

$$C_n = \frac{1}{2\pi} \iint_{BZ} d^2\mathbf{k} \mathcal{B}_{n\mathbf{k}} \quad (17)$$

$$\hat{C}_n = \frac{1}{2\pi} \iint_{\overline{NR}} d^2\mathbf{k} \mathcal{B}_{n\mathbf{k}} \quad (18)$$

$$\tilde{C}_n = \frac{1}{2\pi} \iint_{NR} d^2\mathbf{k} \mathcal{B}_{n\mathbf{k}}. \quad (19)$$

In these three expressions, only the regions of integration differ. For the regular Chern number C_n , the integral is performed over BZ the entire Brillouin zone, while it is done over the region \overline{NR} outside the nodal ring for \hat{C}_n and over the region NR inside the nodal ring for \tilde{C}_n . The first integral running on the whole Brillouin zone refers to the lowest energy band which is characterized through an integer topological number similarly as in the Haldane model, assuming that $3\sqrt{3}t_2 > M$.

As discussed by Haldane in 2004 [22], the partial integrals can still be seen as the Berry flux of particles moving around the closed Fermi surface for each band and can be interpreted as a topological property of the Fermi surface when looking to the semimetal as a Fermi liquid [18], but these integrals are not topological invariants.

Furthermore, the $\mathbf{d}_\mathbf{k}$ vector appearing in the Hamiltonian of Eq. (3) gives us the following well defined map-

ping from the Brillouin Zone to 2-sphere

$$\Phi : BZ \rightarrow S^2 \quad (20)$$

$$\mathbf{k} \mapsto (\theta_{\mathbf{k}}, \varphi_{\mathbf{k}}) \quad (21)$$

where $(\theta_{\mathbf{k}}, \varphi_{\mathbf{k}})$ are the two uniquely defined angles on $S^2 = [0, \pi[\times [0, 2\pi[$ such that

$$\mathbf{d}_{\mathbf{k}} = |\mathbf{d}_{\mathbf{k}}| \begin{pmatrix} \sin \theta_{\mathbf{k}} \cos \varphi_{\mathbf{k}} \\ \sin \theta_{\mathbf{k}} \sin \varphi_{\mathbf{k}} \\ \cos \theta_{\mathbf{k}} \end{pmatrix}. \quad (22)$$

Here, $\varphi_{\mathbf{k}}$ and $\theta_{\mathbf{k}}$ are thus the azimuthal and polar angles of the three-dimensional vector $\mathbf{d}_{\mathbf{k}}$. This map gives us also the following exact expressions (with no approximations)

$$\mathcal{B}_{\downarrow x, -, \mathbf{k}} = -\frac{1}{2} \sin \theta_{\mathbf{k}} (\partial_{k_x} \theta_{\mathbf{k}} \partial_{k_y} \varphi_{\mathbf{k}} - \partial_{k_x} \varphi_{\mathbf{k}} \partial_{k_y} \theta_{\mathbf{k}}) \quad (23)$$

$$\mathcal{B}_{\uparrow x, +, \mathbf{k}} = +\frac{1}{2} \sin \theta_{\mathbf{k}} (\partial_{k_x} \theta_{\mathbf{k}} \partial_{k_y} \varphi_{\mathbf{k}} - \partial_{k_x} \varphi_{\mathbf{k}} \partial_{k_y} \theta_{\mathbf{k}}) \quad (24)$$

$$\mathcal{B}_{\downarrow x, \pm, \mathbf{k}} = \mathcal{B}_{\uparrow x, \pm, \mathbf{k}}. \quad (25)$$

We can then integrate formally by change of variables $\mathbf{k} \rightarrow (\theta, \varphi)$. The Fermi surface formed by the nodal ring can be expressed to a good approximation in these variables by the contour $\theta = \theta_c, \varphi \in [0, 2\pi]$ for a given θ_c fixed between 0 and π depending on the value of r , which defines the position of the nodal ring in the Brillouin zone.

We get by change of variables

$$\begin{aligned} \tilde{C}_{\downarrow x, +} &= \left(\frac{1}{2\pi} \int_0^{2\pi} d\varphi \right) \int_{\theta_c}^{\pi} d\theta \left(+\frac{1}{2} \right) \sin \theta \\ &= \frac{1}{2} [\cos \theta_c + 1] \end{aligned} \quad (26)$$

$$\begin{aligned} \hat{C}_{\uparrow x, -} &= \left(\frac{1}{2\pi} \int_0^{2\pi} d\varphi \right) \int_0^{\theta_c} d\theta \left(-\frac{1}{2} \right) \sin \theta \\ &= \frac{1}{2} (\cos \theta_c - 1) \end{aligned} \quad (27)$$

$$\begin{aligned} C_{\downarrow x, -} &= \left(\frac{1}{2\pi} \int_0^{2\pi} d\varphi \right) \int_0^{\pi} d\theta \left(-\frac{1}{2} \right) \sin \theta \\ &= -1, \end{aligned} \quad (28)$$

which gives us the resulting hall conductivity

$$\begin{aligned} \sigma^{xy} &= \sigma_{\downarrow x, -}^{xy} + \hat{\sigma}_{\uparrow x, -}^{xy} + \tilde{\sigma}_{\downarrow x, +}^{xy} \\ &= \frac{e^2}{h} (\cos \theta_c - 1). \end{aligned} \quad (29)$$

We see that this expression interpolates between $\sigma^{xy} = -\frac{e^2}{h}$ for the topological insulating phase when $\tilde{r} < 3\sqrt{3}t_2 - M$ for which $\theta_c = \pi$ all the way to $\sigma^{xy} = 0$ for the trivial insulating phase when $\tilde{r} > 3\sqrt{3}t_2 + M$ for which $\theta_c = 0$. The nodal ring equivalently navigates from the vicinity of K' towards K when increasing \tilde{r} within the semimetal region such that $3\sqrt{3}t_2 - M < \tilde{r} < 3\sqrt{3}t_2 + M$.

These results do agree with the numerical analysis shown in Fig. 3 which represents the numerical evaluation of Eq. (13). The total Hall conductivity is thus no longer proportional to specific topological invariants in the topological semimetallic phase. However, as shown in Eq. (16), its value can be decomposed into several contributions each having its own topological interpretation, in terms of topological invariant for the $C_{\downarrow x, -}$ term, or in terms of Berry flux accumulated by particles moving around the Fermi surface for the two other terms [22].

Below, we show that the quantized topological response of the lowest band associated to $C_{\downarrow x, -}$ can be measured through circularly polarized light related to a half topological semimetal. Then, we will address the open question of the bulk-edge correspondance in the topological semimetal.

IV. CIRCULARLY POLARIZED LIGHT

Here, we describe the effect of a circularly polarized light field in the plane [7, 9, 10, 26].

We begin with one plane described through a Haldane model within the topological phase to fix the definitions. Within the Dirac approximation, we take the same definitions of the Brillouin zone as in the articles [9, 26], such that the current operator takes the form

$$\hat{J}_{\zeta}(t) = v_F(p_x + A_x(t))\sigma_y - (\zeta p_y + A_y(t))\sigma_x \quad (30)$$

with the velocity $v_F = \frac{3}{2\hbar}ta$ and $\mathbf{p} = (p_x, p_y)$ measures a small deviation from the Dirac points. Here, $\zeta = \pm 1$ at the K and K' respectively such that within the choice of the Brillouin zone the two Dirac points are related through $p_y \rightarrow -p_y$ or more generally $k_y \rightarrow -k_y$. The vector potential due to the classical light source is included through a shift of the momentum. There is a subtlety to mention here within this definition: ζ refers both to the direction of light polarization, right-handed (+) or left-handed (-), and to the Dirac points of interest such that

$$\begin{aligned} \text{Re}A_x &= A_0 \cos(\omega t) \\ \text{Re}A_y &= -\zeta A_0 \sin(\omega t). \end{aligned} \quad (31)$$

The light-matter Hamiltonian can be written in analogy to a spin-1/2 particle where σ^+ and σ^- operators correspond to light-induced hopping terms from one to the other sublattice in the plane [9, 10, 26]. Within the topological phase of the Haldane model, due to the energy conservation and inversion effects between the specific form of eigenstates at the two Dirac points [10, 26], the right-handed circular polarization interacts with one Dirac point and the left-handed circular polarization interacts with the other Dirac point. From the form of the

Dirac Hamiltonian for one layer we also have

$$\begin{aligned}\sigma_x &= \frac{1}{\hbar v_F} \frac{\partial \mathcal{H}}{\partial p_x} \\ \sigma_y &= \frac{1}{\hbar v_F} \frac{\partial \mathcal{H}}{\partial (\zeta p_y)}.\end{aligned}\quad (32)$$

$$\hat{J}_\zeta(t) = (p_x + A_x(t)) \frac{\partial \mathcal{H}}{\hbar \partial (\zeta p_y)} - (\zeta p_y + A_y(t)) \frac{\partial \mathcal{H}}{\hbar \partial p_x}. \quad (33)$$

Since we will evaluate the linear response to second-order in A_0 , as if we just keep the terms in $A_x(t)$ and $A_y(t)$ in this formula, this is equivalent to measure the light-induced response at the Dirac points with here $p_x = p_y = 0$ and to average on all the wavevectors within the Brillouin zone [7]. Therefore, this results in the form of the current operator

$$\hat{J}_\zeta(t) = \frac{1}{2\hbar} A_0 e^{-i\omega t} \left(\frac{\partial \mathcal{H}}{\partial (\zeta p_y)} + \zeta i \frac{\partial \mathcal{H}}{\partial p_x} \right) + h.c. \quad (34)$$

For the Haldane model, this leads to the following transition rates related to the inter-band light-induced transition probabilities [9, 10, 26]

$$\begin{aligned} \Gamma_\zeta(\omega) &= \frac{2\pi}{\hbar} \frac{A_0^2}{2} \left| \langle + | \left(\frac{\partial \mathcal{H}}{\hbar \partial (\zeta p_y)} + \zeta i \frac{\partial \mathcal{H}}{\hbar \partial p_x} \right) | - \rangle \right|^2 \\ &\times \delta(E_l(\mathbf{p}) - E_u(\mathbf{p}) - \hbar\omega). \end{aligned} \quad (35)$$

The symbol ζ only occurs through $\zeta^2 = 1$ which means that it can be dropped at this step of the calculation. It is then important to remind here that we have the correspondences of eigenstates $|+\rangle_K \leftrightarrow |-\rangle_{K'}$ and $|-\rangle_K \leftrightarrow |+\rangle_{K'}$ for the Haldane model such that the crossed terms result in a finite number when measuring $\Gamma_+(\omega) - \Gamma_-(\omega)$. The energy conservation is taken into account through the definition of A_y such that at this step the δ -function is applicable close to both Dirac points; E_l and E_u refer to the lower and upper energy bands with energy $\pm|\mathbf{d}|$ in the Haldane model. These crossed terms are precisely related to the function entering into the quantum Hall response since we can introduce precisely the velocities v^x and v^y of the preceding Section. We show below that it is possible to find a resonance condition for one light polarization only setting $E_u(K) - E_l(K) = \hbar\omega$ with $\mathbf{p} \rightarrow \mathbf{0}$. This implicitly assumes to have a precise knowledge of the energy spectrum from other measures. In this way, we can equivalently (mathematically) integrate on all frequencies since the δ -function is zero when $E_u - E_l \neq \hbar\omega$. Then, this results in a quantized circular dichroic response related to the topological invariant of the lowest and upper bands $C = \mp 1$ [7, 9, 10, 26]

$$\left| \frac{\Gamma_+ - \Gamma_-}{2} \right| = \frac{2\pi}{\hbar} A_0^2 |C|, \quad (36)$$

which can be then equivalently resolved from the information at the Dirac points. It is also relevant to mention

that finding the resonance with the M point(s) or (equivalently Γ -point) this would result in a half-quantized response [10].

Below, we show that the response to circularly polarized light remains meaningful for the topological semimetal, from the K and K' points Dirac theory. For the topological semimetal, within the Dirac approximation for the $d_x(\mathbf{k})$ and $d_y(\mathbf{k})$ terms, the Hamiltonian takes the form

$$\mathcal{H}(\mathbf{p}) = (\hbar v_F (p_x \sigma_x + \zeta p_y \sigma_y) + (\zeta d_z + M) \sigma_z) \otimes \mathbb{I} + r \mathbb{I} \otimes s_x. \quad (37)$$

We introduce precisely identity matrices \mathbb{I} which act in the sublattice and spin Hilbert spaces. Therefore, we can yet write down $\sigma_x \otimes \mathbb{I} = \frac{1}{\hbar v_F} \frac{\partial \mathcal{H}}{\partial p_x} \otimes \mathbb{I}$ and $\sigma_y \otimes \mathbb{I} = \frac{1}{\hbar v_F} \frac{\partial \mathcal{H}}{\partial (\zeta p_y)} \otimes \mathbb{I}$. The current operator then takes the form

$$\hat{J}_\zeta(t) = \left(\frac{1}{2\hbar} A_0 e^{-i\omega t} \left(\frac{\partial \mathcal{H}}{\hbar \partial (\zeta p_y)} + \zeta i \frac{\partial \mathcal{H}}{\hbar \partial p_x} \right) + h.c. \right) \otimes \mathbb{I}. \quad (38)$$

Since we have an identity matrix in the spin sector, within our definitions, this refers to the current of a spin- \uparrow_z or spin- \downarrow_z particle equally. We verify below through justifications from the band structure that since we have an identity operator in the spin space for the current it gives equal currents for a spin- \uparrow_x or spin- \downarrow_x particle.

An important point is to incorporate the energy conservation within the four-energy bands model. It is then useful to write down the light-matter interaction $\delta H_\pm = A_0 e^{\pm i\omega t} \sigma^\pm \otimes \mathbb{I}$ within the four energy bands. Since the light-matter interaction couples bands with the same spin quantum number this implies that at the K -point this will only mediate transitions between bands $n = \downarrow_x, -$ and band $m = \downarrow_x, +$ and separately between bands $n' = \uparrow_x, -$ and band $m' = \uparrow_x, +$. Interestingly, it is possible to find a resonance with both pairs of bands fixing the light frequency such that $\hbar\omega = 2|d_z(K)| = 6\sqrt{3}t_2 + 2M$ for the right-handed wave (+). It is interesting to observe that in the present case, it is possible to fix the resonant condition just with the K Dirac point due to the precise shape of the energy bands in Fig. 1.

Due to the structure of eigenstates in the valley around the K Dirac point, only one of the two light polarizations, e.g. the right-handed polarization, will be able to mediate inter-band transitions similarly to the topological two-bands model. Thus, due to the identification between eigenstates $|\uparrow_z\rangle = \frac{1}{\sqrt{2}}(|\uparrow_x\rangle + |\downarrow_x\rangle)$ and $|\downarrow_z\rangle = \frac{1}{\sqrt{2}}(|\uparrow_x\rangle - |\downarrow_x\rangle)$, we deduce that the inter-band transitions for one spin polarization \uparrow_z or \downarrow_z will then correspond effectively to a half of the sum of the transition rates associated to the two pairs of bands (n, m) and (n', m') respectively, which are in fact equal. Therefore, for the topological semimetal, the response at the K point for the + light polarization is identical to Eq. (35) for each spin polarization $|\uparrow_z\rangle$, $|\downarrow_z\rangle$ or for each pair of bands (n, m) and (n', m') corresponding to spin polarizations $|\downarrow_x\rangle$ and $|\uparrow_x\rangle$ respectively.

At the K' point, the two occupied bands (n and m) at zero temperature have the same spin polarization whereas the two empty bands (n' and m') have now a distinct spin polarization, as shown in Fig. 2. Therefore, to mediate inter-band transitions towards empty states in the quantum limit, this would require to also flip the spin polarization of an electron. Therefore, in the presence of the light field, due to the two-particles ground-state structure at the K' point, this results in $\Gamma_- = 0$ [26]. Hence, if we define circular dichroism for a pair of energy bands, e.g. related to the first (second) and third (fourth) energy bands at the two Dirac points, we also have $\Gamma_- = 0$ for these pairs at finite temperature. It is then useful to analyze the information in Γ_+ at the K point in Eq. (35) through the Berry curvature $F_{p_x p_y}$ mapped onto the 2-sphere [26]. The K Dirac point corresponds to north pole and K' to south pole along the polar angle direction. There is then a simple relation between the Berry curvature in the plane and the pseudo-spin variable [10]

$$F_{p_x p_y} = \frac{2(\hbar v_F)^2}{|E_u - E_l|^2} \cos \theta = \frac{2(\hbar v_F)^2}{|E_u - E_l|^2} \langle \sigma_z(\theta) \rangle \quad (39)$$

where for the topological semimetal, at the K point, $E_u - E_l = E_m - E_n = E_{m'} - E_{n'}$. Therefore, at the K point for a spin polarization \uparrow_z, \downarrow_z or a pair of bands (n, m) and (n', m') we have

$$\left| \frac{\Gamma_+}{2} \right| = \frac{2\pi}{\hbar} A_0^2 \frac{1}{2} \langle \sigma_z(0) \rangle. \quad (40)$$

Since at the K' point, $\Gamma_- = 0$ then this is equivalent to

$$\left| \frac{\Gamma_+ - \Gamma_-}{2} \right| = \frac{2\pi}{\hbar} A_0^2 \frac{1}{2} |\langle \sigma_z(0) \rangle|. \quad (41)$$

Here, σ_z measures the relative density on the two sublattices of the honeycomb lattice resolved at the K Dirac point. In comparison, for the Haldane model, we obtain

$$\begin{aligned} \left| \frac{\Gamma_+ - \Gamma_-}{2} \right| &= \frac{2\pi}{\hbar} A_0^2 \frac{1}{2} |(\langle \sigma_z(0) \rangle - \langle \sigma_z(\pi) \rangle)| \\ &= \frac{2\pi}{\hbar} A_0^2 |\langle \sigma_z(0) \rangle|. \end{aligned} \quad (42)$$

The topological number of the Haldane model on the 2-sphere takes the equivalent form [26, 41]

$$C = \frac{1}{2} (\langle \sigma_z(0) \rangle - \langle \sigma_z(\pi) \rangle). \quad (43)$$

A peculiarity of this topological semimetal is that $\langle \sigma_z(\pi) \rangle = 0$ as a result of the formation of the nodal ring semimetal around K' [19] which is another way to justify why $\Gamma_- = 0$ in this case. The response for one-spin polarization is now halved compared to one topological plane as a result of $\Gamma_- = 0$. The topological semimetal can be characterized in terms of a pair of one-half local

topological markers and π -Berry phases [27] related to the two-spheres' model associated to spin polarizations \uparrow_z, \downarrow_z [19]. In the present situation, the π Berry phase is associated equally to the phase acquired by an electron with spin polarization \uparrow_x in band 2 and by an electron with spin polarization \downarrow_x in band 1, when circling around the K Dirac. A pair of π -Berry phases is also analogous to a pair of π winding numbers [27]. A $\frac{1}{2}$ topological quantized light response is also predicted to occur for the $\nu = \frac{1}{2}$ -fractional quantum Hall effect [42].

If we sum the information on these two spin polarizations (or equally \uparrow_z, \downarrow_z) i.e. on the two pairs of bands (n, m) and (n', m'), we now have

$$\sum_{j=\uparrow, \downarrow} \left| \frac{\Gamma_+ - \Gamma_-}{2} \right| = \frac{2\pi}{\hbar} A_0^2 \cos(\theta = 0). \quad (44)$$

Now, we can establish a precise relation with the quantum Hall response of the lowest energy band in Eq. (29) through

$$C_{\downarrow_x, -} = \frac{1}{2} (\cos(\pi) - \cos(0)) = -\cos(0) = -1. \quad (45)$$

Therefore, we obtain a relation between light and quantum Hall response for the topological semimetal

$$\sum_{j=\uparrow, \downarrow} \left| \frac{\Gamma_+ - \Gamma_-}{2} \right| = \frac{2\pi}{\hbar} A_0^2 |C_{\downarrow_x, -}|. \quad (46)$$

We have reminded above that the light response at the K and K' points for the topological Haldane model reveals the same information as the light response and therefore the quantum Hall response coming from a summation on the whole Brillouin zone [26]. This identification necessitates that the light response functions are continuous and differentiable everywhere. For the topological semimetal, for the intermediate energy bands, the function $F_{p_x p_y}$ flips its sign at θ_c related to the analysis of Sec. III. In this way, the light response from the Dirac points is identical to the quantum Hall response of the semimetal only if $F_{p_x p_y} = 0$ at θ_c for the second band. In the region \overline{NR} , the function $F_{p_x p_y}$ is identical for the two lowest energy bands. Therefore, we must set $\theta_c = \frac{\pi}{2}$ to be sure that the light response from the summation on the whole Brillouin zone would be equivalent to the light responses at the Dirac points. Fixing $\theta_c = \frac{\pi}{2}$, the conductivity response from the second-energy band becomes also zero. This is then another way to justify that the light response at the Dirac points reveals the quantum Hall conductivity of the lowest energy band and therefore the topological invariant, which remains identical for all the range of parameters in Eq. (11).

For $\theta_c = \frac{\pi}{2}$, we also observe that the quantum Hall response coming from \uparrow_x particles in the second-energy band takes the form $\frac{e^2}{h} \widehat{C}_{\uparrow_x, -} = -\frac{1}{2} \frac{e^2}{h}$ which justifies further the introduction of a half topological number for this spin polarization [27]. Similarly, if we now sum the topological number associated to the \downarrow_x particles in the

two energy bands, this also measures $\frac{e^2}{h}(\tilde{C}_{\downarrow x,+} + C_{\downarrow x,-}) = -\frac{1}{2}\frac{e^2}{h}$ and gives a similar interpretation to the other half-topological number. This approach then justifies further the relation between the topological response of the quantum Hall conductivity and $\sum_{j=\uparrow,\downarrow} C_\alpha$ with $|C_\alpha| = \frac{1}{2}$ mentioned in previous publications [18, 19, 27].

When $\tilde{r} < 3\sqrt{3}t_2 - M$, the same light polarization would equally interact with both pairs (n, m) and (n', m') at one Dirac point measuring twice the topological invariant of the lowest band, in agreement with the quantum Hall conductivity. For $\tilde{r} > 3\sqrt{3}t_2 - M$, one pair of bands will interact with one distinct light polarization at each Dirac point. In this case, if we reproduce the steps of the calculation above we now find that $\Gamma_+ - \Gamma_- = 0$ at each Dirac point. In Eq. (33), the two pairs (n, m) and (n', m') are now characterized with different signs of $A_y(t)$ and inverted lower and upper energy eigenstates, for the same Dirac point.

V. BULK-EDGE CORRESPONDANCE

For the Kane-Mele model, as was shown in Fig. 1, the topological semimetal of interest in this paper can be understood as a superposition of two Haldane models associated to each spin polarization towards the axis of the in-plane magnetic field corresponding to the $r\mathbb{I} \otimes s_x$ term (or $\tilde{r}\mathbb{I} \otimes s_x$ term in the presence of interactions) in the Hamiltonian of Eq. (3). This magnetic field of small amplitude polarizes the system into two subsystems which are independent of each other as long as the \mathbb{Z}_2 symmetry of the Hamiltonian is preserved.

As shown in the upper panel of Fig. 4, these two subcopies of the Haldane model are of the same topological nature in the sense that the lower bands have the same Berry curvature and hence the same Chern number, but the bands of the two sub systems are not filled evenly. The second band of the \downarrow_x population is partially filled while the first band of the \uparrow_x population is partially filled symmetrically to the \downarrow_x population. As long as the \mathbb{Z}_2 symmetry of the system is preserved, the two subsystems are well defined and the lower band of the \uparrow_x population does not mix to the upper band of the \downarrow_x population, and no gap is opened in the band structure.

The topological nature of this semimetal comes from the fact that each of the spin subsystem acts as if its chemical potential was shifted by $\pm r$ from its half-filling value, which leads for the bands to be either emptied or filled in a symmetric way between the two subsystems. This does not change however the topological nature of the bands themselves which keep their Berry curvature and their resulting Chern number. The semimetallic behavior thus does not come from a transition from a trivial to a topological insulator for which the topological nature of the band is not well defined. The topological nature of the bands is well defined here in terms of Chern number, but in the given context, the resulting band structure is gapless when taking the two spin populations together.

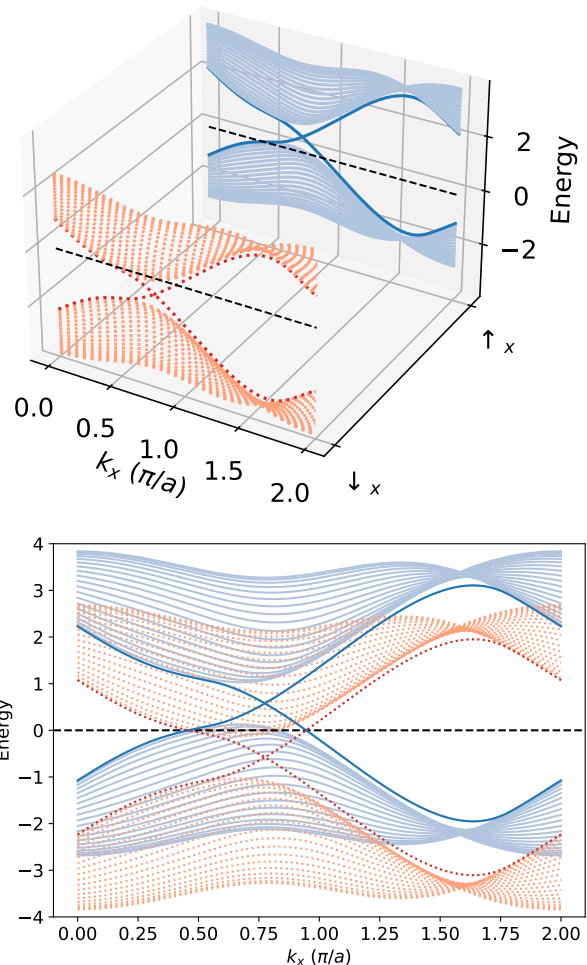


Figure 4. Color online: (Above) One-dimensional energy bands of the topological semimetal showing the two underlying band structures of opposite spin polarization, with the spin polarization shown in the third direction. (Bottom) Resulting energy bands in the momentum-Energy axis. The parameters chosen for all panels are $M = 3\sqrt{3}t/4$, $r = t/\sqrt{3}$, $t_2 = t/3$ with $a = 1$.

A way to probe this topological system is using spin-resolved ARPES measurement which should allow us to measure the two band structures of the upper panel of Fig. 4 separately and to resolve the bands lying inside the gap of each spin population, justifying hence the topological nature of this semimetal. However, the overall system will not develop a total quantized Hall conductance due to the presence of the bulk modes corresponding to the Fermi surface of each spin population, which, in a Landauer-Büttiker approach of the conductance, will result in an amplified value of the Hall conductance of the sample, not equal to the bulk value derived in Eq. (29). Hence, spin resolved ARPES measurements appear as the most simple and decisive way to probe the topological nature of this semimetal.

Another way to probe the topological nature of this semimetal is using spin-polarized transport measurements at chemical potential μ which satisfies $|\mu \pm r| <$

$|M - 3\sqrt{3}t_2|$. Indeed, the spin polarization of the system in the x direction is a well defined quantum number and in such a regime for the chemical potential, the mesoscopic Hall conductance of one spin population is quantized due to the unique presence of spin-polarized edge modes while the conductance of the other population is non quantized due to the presence of spin-polarized bulk modes at this regime of chemical potential. If we consider the graphic representations of the energy bands in Fig. 4, the system can thus be seen in this regime of chemical potential as a half-topological semimetal: one spin population is in the topological insulating phase while the other is in a metallic regime. We also emphasize here that the presence of a quantized conductance at the edges for one spin-population polarized along x direction is also equivalent to a $\frac{1}{2} - \frac{1}{2}$ conductance for the two spin polarizations along z direction which is precisely at the heart of the bulk-edge correspondence interpretation for the bilayer model [19, 27].

Similarly, spin resolved ARPES measurements on a generic spin Hall system should allow us to retrieve the band structure of each spin population independently, and thus to characterize the topological nature of each spin population on its own. This approach should allow us for example to exhibit the two band structures of the upper panel of Fig. 1 separately and to identify the topological nature of the spin Hall phase for the case of the Kane-Mele model. From Sec. III, for the topological semimetal, we also observe the equality

$$\hat{C}_{\uparrow x,-} - \tilde{C}_{\downarrow x,+} = C_{\downarrow x,-}, \quad (47)$$

which is valid for all the ranges of applicability of Eq. (11) and formulates a correspondence between the integer \mathbb{Z} topological invariant of the lowest-energy band and a \mathbb{Z}_2 spin topological number for the second-energy band.

This approach consisting in visualizing the band structure into distinct sectors of symmetry of the system brings powerful insight into the common definitions of the quantum Hall \mathbb{Z} and of the quantum spin Hall \mathbb{Z}_2 invariants defined commonly in the literature. The general case would consist in a system made of several subsystems corresponding to distinct symmetry sectors of the symmetry of the system, and we can consider the system to be in a topological phase as long as one of the subsystems is itself in a topological phase. This tells us why the \mathbb{Z} invariant is not relevant for the quantum spin Hall phase, because the two subsystems are of opposite Chern while still being separately in a topological phase, so that having the sum of their invariants being zero cannot help characterizing the topological nature of the phase. The \mathbb{Z}_2 invariant defined as the difference of the two invariants of the subsystems helps us finding a non zero topological invariant but this invariant is very much restricted to the precise context of subsystems being of opposite topology. Instead, at least on the theoretical level, one can consider more generally systems for which the symmetry sectors behave independently from each other and have their own topology, and neither the commonly defined \mathbb{Z} or \mathbb{Z}_2 can

help characterizing the topological phase entirely, as for example is the case of the following system

$$\mathcal{H}_{\mathbf{k}} = \begin{pmatrix} d_x(\mathbf{k}) & & \\ & d_y(\mathbf{k}) & \\ M + (t_2 + \tilde{t}_2) \sum_j \sin(\mathbf{k} \cdot \mathbf{b}_j) & & \end{pmatrix} \cdot \boldsymbol{\sigma} \otimes \mathbb{I} \\ + (t_2 - \tilde{t}_2) \sum_j \sin(\mathbf{k} \cdot \mathbf{b}_j) \sigma_z \otimes s_z \quad (48)$$

This model can realize different topological phases. This system would be in fact in a topological phase as long as $\left| \frac{M}{3\sqrt{3}t_2} \right| < 1$ or $\left| \frac{M}{3\sqrt{3}\tilde{t}_2} \right| < 1$. The case of the Kane-Mele model and the quantum spin Hall phase would correspond to $\tilde{t}_2 = -t_2$ for which the \mathbb{Z}_2 spin topological number is relevant to characterize the topological phase, and the case $\tilde{t}_2 = t_2$ would correspond to the usual bilayer Haldane model for which the \mathbb{Z} number is relevant to characterize the topological phase. However, neither of these two invariants can help to characterize entirely the topological phase in the general context of $t_2 \neq \pm\tilde{t}_2$. Hence, from general aspects, the topological phase of the system needs to be characterized for each symmetry sector independently, each having its own Chern number.

VI. CONCLUSION

To summarize, we have derived the quantum Hall conductivity of the recently identified two-dimensional topological nodal ring semimetal on the honeycomb lattice and obtained two distinct responses: a topological response of the lowest energy band which reveals an integer \mathbb{Z} topological invariant and two Fermi surface terms from the two partially filled bands of opposite spins. We emphasize here that the Kubo formula is well applicable in the presence of a band-crossing effect as a result of orthogonality between spin quantum numbers of energy bands at the chemical potential. This orthogonality is also at the heart of the stability and protection of this phase of matter towards disorder and interaction effects which would only slightly dress the effect of the in-plane magnetic field. The \mathbb{Z} topological invariant $C_{\downarrow x,-}$ associated to the lowest-energy band is also mathematically identical to a \mathbb{Z}_2 spin Chern number $\hat{C}_{\uparrow x,-} - \tilde{C}_{\downarrow x,+}$ for the partially filled bands. The specificity of the topological semimetal phase resides in the occurrence of gap closing region at the Fermi energy due to crossing between two bands which in the present case is also characterized through a \mathbb{Z}_2 spin Chern number. We have then evaluated the response to circularly polarized light, which is an equivalent marker of the topological response and of the quantum Hall conductivity for the Haldane model, and showed how this can reveal the topological response of the quantum Hall conductivity for the lowest band of the topological semimetal from the Dirac points.

This approach for the light-matter interaction resolved in the two Dirac valleys is also equivalent to a measure of the quantum Hall conductivity in the situation of a

pair of one-half topological numbers related to the two-spheres' model with a sphere associated to a \uparrow_z or \downarrow_z spin polarization. We have then justified that the formation of a half-topological semimetal can also be understood as one spin population along x direction being in the topological insulating phase while the other is in a metallic regime resulting in a conductance at the edges quantized for one spin-polarization only. The quantized edge mode then has a $1/2$ probability to be in the \uparrow_z, \downarrow_z state associated to the original basis of the Hamiltonian. These results can be verified through spin-polarized transport at the edges and spin-polarized ARPES. These protected topological semimetals present then two different flows of charges, associated to a two-dimensional Fermi liquid in the bulk and a one-dimensional channel at the edge. It is also interesting to mention here that one-half topo-

logical numbers also find applications for the physics of interacting topological superconducting p-wave wires [43] and the physics of Majorana fermions [27, 44].

The bulk-edge correspondence yet hides some mysteries related to the classification of these robust, but at same time fragile, two-dimensional topological semimetals which may be addressed in future articles. Similarly, an interesting question may address the evolution of the present findings towards three dimensions.

We acknowledge useful discussions with Joel Hutchinson, Andrej Mesaros and Michel Ferrero for interesting discussions. This work was supported by the french ANR BOCA and the Deutsche Forschungsgemeinschaft (DFG), German Research Foundation under Project No. 277974659. Sariah Al Saati thanks Ecole Polytechnique for funding his PhD thesis.

-
- [1] M. Z. Hasan and C. L. Kane, *Reviews of Modern Physics* **82**, 3045 (2010).
- [2] K. v. Klitzing, G. Dorda, and M. Pepper, *Physical Review Letters* **45**, 494 (1980).
- [3] D. J. Thouless, M. Kohmoto, M. P. Nightingale, and M. den Nijs, *Physical Review Letters* **49**, 405 (1982).
- [4] Y. Hatsugai, *Physical Review Letters* **71**, 3697 (1993).
- [5] Y. Hatsugai, *Physical Review B* **48**, 11851 (1993).
- [6] M. Kohmoto, *Annals of Physics* **160**, 343 (1985).
- [7] D. T. Tran, A. Dauphin, A. G. Grushin, P. Zoller, and N. Goldman, *Science Advances* **3** (2017).
- [8] L. Asteria, D. T. Tran, T. Ozawa, M. Tarnowski, B. S. Rem, N. Flaschner, K. Sengstock, N. Goldman, and C. Weitenberg, *Nature Physics* **15**, 449 (2019).
- [9] P. W. Klein, A. Grushin, and K. Le Hur, *Phys. Rev. B* **103**, 035114 (2021).
- [10] K. Le Hur, *Phys. Rev. B* **105**, 125106 (2022).
- [11] M. Dyakonov and V. Perel, *Soviet Journal of Experimental and Theoretical Physics Letters* **13**, 467 (1971).
- [12] S. Murakami, N. Nagaosa, and S.-C. Zhang, *Science* **301**, 1348 (2003).
- [13] C. L. Kane and E. J. Mele, *Physical Review Letters* **95**, 226801 (2005).
- [14] C. L. Kane and E. J. Mele, *Physical Review Letters* **95**, 146802 (2005).
- [15] B. A. Bernevig and S.-C. Zhang, *Physical Review Letters* **96**, 106802 (2006).
- [16] L. Sheng, D. N. Sheng, C. S. Ting, and F. D. M. Haldane, *Phys. Rev. Lett.* **95**, 136602 (2005).
- [17] L. Fu and C. L. Kane, *Phys. Rev. B* **76**, 045302 (2007).
- [18] K. Le Hur and S. Al Saati, *Physical Review B* **107**, 165407 (2023).
- [19] J. Hutchinson and K. Le Hur, *Communications Physics* **4**, 144 (2021).
- [20] F. D. M. Haldane, *Physical Review Letters* **61**, 2015 (1988).
- [21] X. Feng, J. Zhu, W. Wu, and S. A. Yang, *Chinese Physics B* **30**, 107304 (2021).
- [22] F. D. M. Haldane, *Physical Review Letters* **93**, 206602 (2004).
- [23] B. Fu, J.-Y. Zou, Z.-A. Hu, H.-W. Wang, and S.-Q. Shen, *npj Quantum Materials* **7**, 94 (2022).
- [24] Y. Guo, Z. Lin, J.-Q. Zhao, J. Lou, and Y. Chen, *Scientific Reports* **9**, 18516 (2019).
- [25] L.-H. Hu, C. Guo, Y. Sun, C. Felser, L. Elcoro, P. J. W. Moll, C.-X. Liu, and B. A. Bernevig, *Physical Review B* **107**, 125145 (2023).
- [26] K. Le Hur, *Review Submitted to Physics Reports, Elsevier, September 2023*, arXiv:2209.15381 (2022).
- [27] K. Le Hur, arXiv:2308.14062, accepted in *Physical Review B*.
- [28] P. Cheng, P. W. Klein, K. Plekhanov, K. Sengstock, M. Aidelsburger, C. Weitenberg, and K. Le Hur, *Phys. Rev. B(R)* **100**, 081107(R) (2019).
- [29] J.-H. Zheng and W. Hofstetter, *Phys. Rev. B* **195434**, 195434 (2018).
- [30] T. H. Hsieh, H. Ishizuka, L. Balents, and T. Hughes, *Phys. Rev. Lett.* **116**, 086802 (2016).
- [31] T. Shoman, A. Takayama, T. Sato, S. Souma, T. Takahashi, T. Oguchi, K. Segawa, and Y. Ando, *Nature Communications* **6**, 6547 (2015).
- [32] Z. Wang, D. Ki, H. Chen, H. Berger, A. H. MacDonald, and A. F. Morpurgo, *Nature Communications* **6**, Article number:8339 (2015).
- [33] P. Tiwari, S. K. Srivastav, S. Ray, T. Das, and A. Bid, *ACS Nano* **15**, 916 (2020).
- [34] J. W. McIver, B. Schulte, F.-U. Stein, T. Matsuyama, G. Jotzu, G. Meier, and A. Cavalleri, *Nature Physics* **16**, 38 (2020).
- [35] G. W. Semenoff, *Physical Review Letters* **53**, 2449 (1984).
- [36] J. Hutchinson, P. W. Klein, and K. Le Hur, *Phys. Rev. B* **104**, 075120 (2021).
- [37] I. Titvinidze, J. Legendre, K. Le Hur, and W. Hofstetter, *Phys. Rev. B* **105**, 235102 (2022).
- [38] W. Wu, S. Rachel, W.-M. Liu, and K. Le Hur, *Phys. Rev. B* **85**, 205102 (2012).
- [39] M. Hohenadler, T. C. Lang, and F. F. Assaad, *Phys. Rev. B* **106**, 100403 (2011).
- [40] M. V. Berry, *Proceedings of the Royal Society A, Mathematical Physical and Engineering Sciences* **392**, 1802 (1984).
- [41] L. Henriot, A. Sclocchi, P. P. Orth, and K. Le Hur, *Phys. Rev. B* **95**, 054307 (2017).

- [42] C. Repellin and N. Goldman, *Phys. Rev. Lett.* **122**, 166801 (2019).
- [43] F. del Pozo, L. Herviou, and K. Le Hur, *Phys. Rev. B* **107**, 155134 (2023).
- [44] E. Bernhardt, B. Chung Hang Cheung, and K. Le Hur, , arXiv:2309.03127.